Published in final edited form as:

Circ Res. 2021 November 12; 129(11): 1021–1035. doi:10.1161/CIRCRESAHA.121.319482.

Matricellular Protein Cilp1 Promotes Myocardial Fibrosis in Response to Myocardial Infarction

Qing-Jun Zhang[1,#], **Yu He**[2,#], **Yongnan Li**[3,#], **Huali Shen**[4], **Ling Lin**[4], **Min Zhu**[1], **Zhaoning Wang**[5], **Xiang Luo**[1], **Joseph A. Hill**[1,5], **Dian Cao**[1], **Richard L. Luo**[1], **Raymond Zou**[1], **John McAnally**[5], **Jun Liao**[6], **Pietro Bajona**[7,8], **Qun S. Zang**[9], **Yonghao Yu**[10], **Zhi-Ping Liu**[1,5]

[1]Internal Medicine-Cardiology Division, UT Southwestern Medical Center, Dallas, TX 75390

[2]Department of Clinical Laboratory, First Affiliated hospital of Guangxi Medical University, No. 6 Shuangyong Road, Nanning, Guangxi, 530021, China

[3]The Sixth General Surgery, Biliary & Vascular surgery, Shengjing Hospital of China Medical University, No. 36 San Hao Street, Heping District, Shenyang, Liaoning, 110004, China

[4]Institutes of Biochemical Science, Fudan University, Shanghai, 200032, China

[5]Department of Molecular Biology, UT Southwestern Medical Center, Dallas, TX 75390

[6]Department of Bioengineering, University of Texas at Arlington, Arlington, TX 76010

[7]Department of Cardiovascular and Thoracic Surgery, UT Southwestern Medical Center, Dallas, TX 75390

[8]Allegheny Health Network-Drexel University College of Medicine, Pittsburgh, PA 15212

[9]Burn & Shock Trauma Research Institute, Department of Surgery, Stritch School of Medicine, Loyola University, Maywood, IL 60153

[10]Department of Biochemistry, UT Southwestern Medical Center, Dallas, TX 75390

Abstract

Rationale: Cartilage intermediate layer protein 1 (Cilp1) is a secreted extracellular matrix (ECM) protein normally associated with bone and cartilage development. Its function and mechanism of action in adult heart disease remain elusive.

Objective: To establish the function and mechanism of action of Cilp1 in post-myocardial infarction (MI) cardiac remodeling.

Methods and Results: We investigated the expression of Cilp1 in mouse models of pathological cardiac remodeling and human heart failure patients. Cilp1 was expressed

Address correspondence to: Dr. Zhi-Ping Liu, University of Texas Southwestern Medical Center, Internal Medicine and Molecular Biology, 6000 Harry Hines Blvd, Dallas, Texas 75390, United States, Tel: 214-6481485, Zhi-Ping.Liu@UTsouthwestern.edu.
[#]These authors contributed equally.

DISCLOSURES
None.

predominantly in cardiac fibroblasts and upregulated in response to cardiac injury and in the heart and blood of heart failure patients. We generated Cilp1 knock out (KO) and transgenic (Tg) mice with N-terminal half of the protein (NCilp1) overexpressed in myofibroblasts. *Cilp1* KO mice had better cardiac function, reduced number of immune cells and myofibroblasts, and enhanced microvascular survival after MI compared to wild-type (WT) littermates. Conversely, NCilp1-Tg mice had augmented loss of cardiac function, increased number of myofibroblasts and infarct size after the MI injury. RNA-seq and gene ontology analysis indicated that cell proliferation and mTORC1 signaling were downregulated in KO hearts compared to WT hearts. *In vivo* BrdU labeling and immunofluorescence staining showed that myofibroblast proliferation in the *Cilp1* KO heart was downregulated. Biaxial mechanical testing and ECM gene expression analysis indicated that while MI caused significant stiffness in WT hearts it had little effect on KO hearts. Upregulation of collagen expression after MI injury was attenuated in KO hearts. Recombinant CILP1 protein or NCilp1-conditioned medium promoted proliferation of neonatal rat ventricular cardiac fibroblasts via the mTORC1 signaling pathway.

Conclusions: Our studies established a pathological role of Cilp1 in promoting post-MI remodeling, identified a novel function of Cilp1 in promoting myofibroblast proliferation, and suggested that Cilp1 may serve as a potential biomarker for pathological cardiac remodeling and target for fibrotic heart disease.

Graphical Abstract

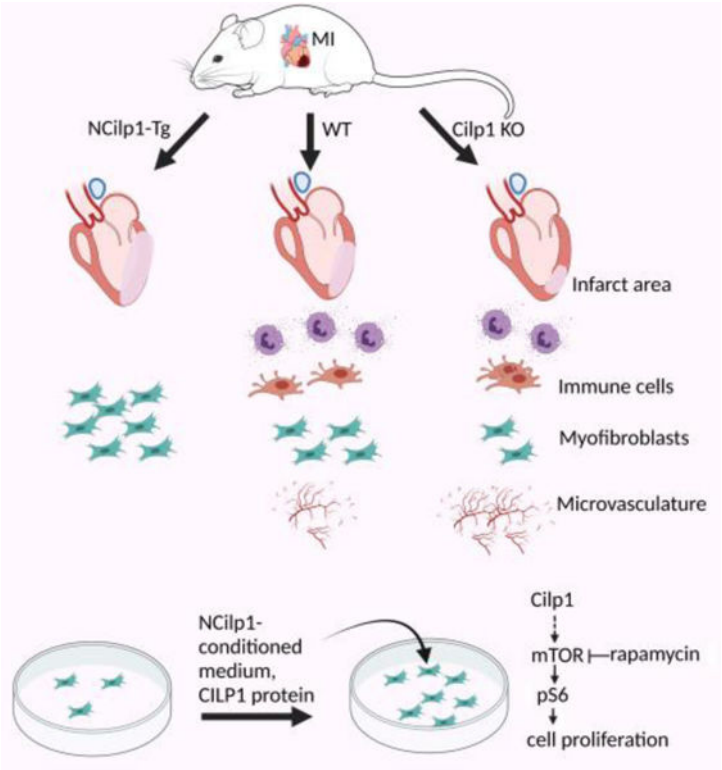

Keywords

Basic Science Research; Cell Signaling/Signal Transduction; Fibrosis; Ischemia; Myocardial Biology

INTRODUCTION

Myocardial fibrosis is the common pathological outcome of nearly all forms of heart disease including myocardial infarction (MI) and a major risk factor for heart failure [1, 2]. Myocardial fibrosis is irreversible. As the adult heart has limited regenerative capacity, a stable scar must quickly form to prevent ventricular wall rupture. Fibrosis is characterized by excessive deposition of a collagen-rich extracellular matrix (ECM) [3]. The characteristics of the scar including its molecular composition and mechanics are the critical determinants of subsequent pathological remodeling, which can change the size, shape, and physiology of the heart, ultimately leading to heart failure. Great efforts in the past have been focused on repopulating the scar tissue with either endogenously or exogenously derived-cardiomyocytes, and on therapies targeting inflammatory mediators and myofibroblasts [4567–10]. These efforts have not yet led to effective therapies [11, 12]. On the other hand, genetic modification and/or pharmacological targeting of ECM components have been shown to alter the scar characteristics and partially restore the contractile and electrical conduction properties of the scar [13]. Myofibroblast is the principal cell type for post-MI ECM. Using the natural reparative processes of myofibroblast to modify properties of the infarct scar is emerging as an exciting therapeutic avenue [8, 13]. However, the ability to therapeutically modify cardiac scar tissue is still limited by a lack of knowledge of what constitutes benefit. Research is much needed to gain insight into the molecular determinants of the fibrosis-driven ECM.

Cartilage intermediate layer protein 1 (Cilp1) is a matricellular protein, originally found secreted predominantly from chondrocytes in articular cartilage [14] and is implicated in common musculoskeletal disorders, including osteoarthritis and lumbar disc degeneration [15]. Cilp1 is a large protein with 1184 amino acid residues and is cleaved into N- and C-terminal parts at amino acid 721 upon secretion [14, 16, 17]. The C-terminal portion is homologous to nucleotide pyrophosphatase phosphodiesterase (NPP) but with no intrinsic NPP activity [16]. The N-terminal part (NCilp1) contains a highly conserved thrombospondin type 1 repeat domain (TSR) known to bind Tgfβ. Binding of Cilp1 to Tgfβ blocks the Tgfβ/Smad signaling and inhibits transcriptional activation of cartilage matrix genes in nucleus pulposus cells in vitro and matrix deposition in vivo [18]. Cilp1 is also expressed in the heart and implicated in cardiac extracellular matrix remodeling [19–22]. Cilp1 is significantly elevated in post-mortem human infarct tissues and in aortic valve stenosis patients [19]. Cilp1 was shown, paradoxically in the same study, decreased in the circulation of heart failure patients even though it was upregulated in the infarcted heart tissues [23]. Cilp1 is also significantly upregulated in mouse hearts undergoing pathological ventricular remodeling induced by MI, trans aortic constriction (TAC), or AngII-treatment [19, 20, 24]. Whether upregulation of Cilp1 in diseased heart plays a protective role against or pathological role driving adverse remodeling remains elusive. One study suggested that Cilp1 may play an anti-fibrosis role

in a mouse model of pressure-overload induced by TAC [20]. Recombinant Cilp1 protein was also shown to inhibit Tgfβ1-induced expression of smooth muscle alpha-actin (αSMA) in vitro [19, 21], suggesting it may inhibit myofibroblast differentiation and myocardial fibrosis during pathological cardiac remodeling.

Here, we present evidence supporting a role of Cilp1 in promoting pathological cardiac remodeling and myocardial fibrosis. Our studies revealed that Cilp1 was expressed predominantly in cardiac fibroblasts and upregulated in animal models of adverse cardiac remodeling and in blood of heart failure patients. We generated *Cilp1* knock out (KO) mice from commercial *Cilp1*$^{fl/fl}$ mice and transgenic (Tg) mice with NCilp1 overexpressed in myofibroblasts. Deletion of *Cilp1* in mice attenuated adverse cardiac remodeling caused by MI and TAC injuries. *Cilp1* KO mice showed reduced post-MI inflammation, reduced number of myofibroblasts, and enhanced survival of microvasculature compared to WT littermates. Conversely, NCilp1-Tg mice had exacerbated post-MI remodeling with reduced cardiac function and increased number of myofibroblasts and infarct size. Further mechanistic studies indicated that recombinant CILP1 protein or conditional medium containing secreted NCilp1 promoted proliferation of neonatal ventricular cardiac fibroblasts (NRV cFbs) in vitro via the mTORC1 signaling pathway. Cilp1 also promoted proliferation of adult cFbs. The mTORC1 signaling was upregulated in proliferating myofibroblasts of infarcted heart in response to MI, which was attenuated in infarcted *Cilp1* KO hearts compared to WT hearts. Our study identified a novel function of Cilp1 in promoting myofibroblast proliferation under pathological conditions that may underly the mechanism by which Cilp1 promotes post-MI remodeling and suggested it may be a potential biomarker for adverse cardiac remodeling and therapeutic target in pathological cardiac remodeling and fibrosis.

METHODS

Data Availability.

A description of all materials and detailed methods is provided in the Supplemental Materials and are available from the corresponding author upon request.

Statistical method.

Data are presented as Mean ± SEM. n numbers are biological replicates. At least 3 independent experiments and 2~3 samples/experiment/group were performed for each assay. Shapiro-Wilk test was used to test normality. 0.05 threshold was assumed. A parametric t-test was made when the dataset met the normality test. For dataset that did not meet normality test, non-parametric Mann-Whitney test was used. Changes were considered to be significant when $p<0.05$. Statistical analysis was performed with Graphpad Prism.

RESULTS

Cilp1 is differentially expressed in the MI-heart compared to the sham-heart and absent in CCl_4-induced liver fibrosis.

In search for molecular mechanisms underlying the irreversible cardiac fibrosis, we performed a large-scale quantitative proteomics of infarcted mouse hearts, fibrotic livers-induced by CCl_4 [25], and bleomycin-treated lungs [26], along with respective sham and vehicle-treated control tissues (Figure 1). Unlike injury induced myocardial fibrosis that is irreversible, chemical induced fibrosis of the liver and lung is reversible/partially reversible once the inciting chemicals are removed. About 4600 quantifiable proteins were identified in each sample. There were approximately 800 differentially expressed proteins in the infarcted heart (>=2-fold change) compared to the sham-heart with Cilp1 being the most differentially expressed one (Figure 1A). Gene ontology (GO) analysis (DAVID, NIH) suggested that proteins involved in ECM biology were among the top ones (Figure 1B). We have identified 210 ECM proteins (~25% of total differentially expressed proteins) including proteins involved in collagen biosynthesis such as Col1, Col3, Col5, and P3H1. ECM proteins uniquely found in the heart include lysyl oxidases (Lox) and Lox-like proteins (Loxl1, Loxl2, Loxl3) (Figure 1C). Lox and Lox-like proteins are enzymes responsible for crosslinking collagens. Interestingly Loxl2 and Loxl3 were upregulated only in the infarcted heart and had low expression levels or no change in the CCl_4-induced fibrotic liver (Figure 1C). CCl_4-induced liver fibrosis is reversible once CCl_4 is removed. Galectin3, an emerging marker for chronic heart failure [27], and growth factors Tgfβ1 and Bmp1, are also among the differentially expressed proteins in our dataset. These results demonstrated the superiority of our protocol; it identifies not only the abundant ECM structural proteins such as collagens but also growth factors that have low-expression levels. In addition to Cilp1, differentially expressed proteins in the heart tissue also included Ltbp2, Thbs2, and Aspn, which are involved in the Tgfβ signaling.

Cilp1 is upregulated in response to heart injuries and expressed in the cardiac fibroblast.

We further investigated the expression of Cilp1 in diseased mouse and human hearts. Cilp1 was upregulated in both remote area (RA) and infarct area (IA) at post-MI day 3 and 7 (Figure 2A). Interestingly, Cilp1 was transiently downregulated in the IA at post-MI day1 even though its expression was upregulated in the RA. Cilp1 was also upregulated in mouse hearts subjected to TAC (Figure 2B), which induces cardiac hypertrophy and interstitial fibrosis [28]. BAPN (β-aminopropionitrile) is lysyl oxidase inhibitor that has been shown to reduce myocardial fibrosis in various animal models of heart disease [29–31]. TAC-induced upregulation of Cilp1 can be reduced in the presence of BAPN (Figure 2B). To identify the cellular source of upregulated Cilp1 in the heart, we examined the expression pattern of Cilp1 in three publicly available single cell RNA-seq (scRNA-seq) datasets using a t-distributed stochastic neighbor embedding (t-SNE) method [32]: 1) Tabula Muris containing single-cell transcriptomic data of 20 mouse organs [33]; 2) E-MTAB-6173 containing single-cell transcriptional profiles of mouse non-cardiomyocytes [34]; and 3) GSE97117 containing scRNA-seq data of hearts from a $Pln^{R9C/+}$ and a WT control mouse [35]. $Pln^{R9C/+}$ mouse has a cardiac fibrosis phenotype due to R9C mutation in phospholamban [36]. Cilp1 was expressed predominantly in cardiac fibroblasts (Online Figure IA and IB)

and was upregulated in fibroblasts of *Pln*$^{R9C/+}$ heart (Online Figure IC). We fractionated cardiomyocytes and non-cardiomyocytes from sham and TAC hearts. Cilp1 expression was also observed predominantly in non-cardiomyocyte fraction and further upregulated after TAC (Figure 2C). Cilp1 was also expressed in neonatal rat ventricular cardiac fibroblast (NRV cFbs) and adult cFbs and was upregulated in response to Tgfβ1 (Figure 2D). A recent report with single cell RNA-seq of AngII-induced fibrotic hearts also indicated that Cilp1 is expressed in cardiac fibroblasts [24].

Cilp1 was shown previously to be upregulated in post-mortem human infarct tissues and in aortic valve stenosis patients [19]. Consistently, we also observed upregulation of Cilp1 in hypertrophic cardiomyopathy (HCM) patients' hearts (Figure 2E). Because of Cilp1 is a secreted protein, we tested if it can be detected in the circulation of heart failure patients and therefore may be used as a potential biomarker. We performed ELISA analysis of CILP1 in sera of normal (ctl) and dilated cardiomyopathy (DCM) patients with unknown etiology (Online Table I). CILP1 was significantly upregulated in the blood of DCM patients compared to that of controls (Figure 2F). As Cilp1 was downregulated in diseased mouse hearts treated with anti-fibrosis agent (Figure 2B), we tested if this could be the case in human. Downregulation of CILP1 was indeed observed in human hearts after use of left ventricular assisted device (LVAD) compared to those before LVAD (Online Figure II).

Cilp1-deletion attenuates pathological cardiac remodeling.

Cilp1 KO mice were viable and fertile with no overt phenotypes at baseline. We subjected KO and WT littermates to the MI surgery. Loss of Cilp1 resulted in a better cardiac function with significantly greater percent of fractional shortening (FS%) (Figure 3A) and smaller LVESD (Figure 3B) compared to WT hearts. Although LVEDD in KO hearts was also reduced, it was not significant (Figure 3C). Inactivation of *Cilp1* also resulted in a reduced infarct size upon MI (Figure 3D-E). *Cilp1* KO mice also had reduced HW/BW compared to WT mice (Online Figure III). We also subjected *Cilp1* KO and WT littermate to TAC surgery. *Cilp1* KO mice showed attenuated hypertrophic remodeling with better cardiac function (Figure 3F-H), reduced HW/BW ratio (Figure 3I) and cardiomyocyte areas (Figure 3J), and expression of hypertrophic (Figure 3K) and fibrotic maker Periostin (Postn) (Figure 3L). *Cilp1* KO hearts also had less post-TAC fibrosis (Figure 3M).

Cilp1 promotes post-MI inflammation and myofibroblast proliferation.

We next focused on the cellular phenotypes of MI injury. Post-MI cardiac remodeling consists of three overlapping stages, early inflammation (post-MI day1 to day 3 in mice), fibroblast proliferation and differentiation to myofibroblasts (day 3–7), and maturation of fibrotic scars (>day 7) [37, 38]. Inflammatory cells such as neutrophils marked by Ly6G and macrophages marked by CD68 were low/absent at baseline in both WT and *Cilp1* KO hearts (Online Figure IVA-B), they were upregulated in WT infarcted hearts at post-MI day 3 compared to day 1 and significantly attenuated in *Cilp1* KO hearts (Figure 4-B). Similarly, few aSMA+ myofibroblasts were observed at baseline in both WT and *Cilp1* KO hearts (Online Figure 4C), they were upregulated at post-MI day 7 compared to day 3 in WT infarcted hearts whereas this upregulation was significantly reduced in *Cilp1* KO hearts (Figure 4C). Interestingly, microvasculature stained with endothelial cell marker

CD31 was downregulated in post-MI day 7 compared to day 3 in WT hearts whereas remained similar between post-MI day 3 and 7 in *Cilp1* KO hearts (Figure 4D), suggesting deletion of *Cilp1* resulted in a better survival of microvasculature. No difference of the vimentin$^+$ mesenchymal cells or CD31$^+$ endothelial cells were observed between WT and *Cilp1* KO hearts at baseline (Online Figure IVD-E), suggesting the different amounts of myofibroblast and microvasculature in the infarcted WT and *Cilp1* KO heart were the result of injury-induced remodeling.

We performed gene profiling of sham and post-MI day 3 WT and Cilp1 KO hearts using RNA-seq assays (Figure 5A). Gene ontology analysis of >2-fold differentially expressed genes between *Cilp1* KO IA and WT IA indicated that cell proliferation and inflammation were among the top downregulated molecular processes in the KO hearts (Figure 5B). We confirmed the downregulation of several top differentially expressed inflammatory cytokines and cell cycle genes in infarcted KO hearts over infarcted WT hearts by qRT-PCR with independent tissue samples (Figure 5C-D). To test if downregulation of aSMA$^+$ cells in the infarcted KO hearts was due to cell proliferation, WT and KO hearts were pulse-labeled with BrdU at post-MI day 3 and 7 for 4 hrs before being fixed for histological analysis. Heart sections were co-stained with antibodies against BrdU and αSMA (Figure 5E). BrdU-labeled aSMA$^+$ cells in the KO IA were significantly downregulated compared to WT hearts at post-MI day 3 and were similar to WT hearts at post-MI day 7 (Figure 5F). Consequently, aSMA$^+$ cells in infarcted KO hearts at post-MI day 7 were significantly less than WT hearts (Figure 5G). As αSMA also stains smooth muscle cells (SMCs) around vasculature, we co-stained infarcted hearts with αSMA and vimentin that stains noncardiomyocytes including the fibroblast [24]. Majority of αSMA$^+$ cells overlapped with vimentin$^+$ cells in the IA (Online Figure VA). Proliferation of vimentin$^+$ fibroblasts of KO hearts was also downregulated at post-MI day 3 compared to WT hearts as assayed by BrdU-labeling (Online Figure VB). These results suggested that myofibroblasts in infarcted Cilp1 KO hearts were downregulated compared to WT hearts and likely due to reduced cell proliferation.

Cilp1 promotes myofibroblast proliferation via the mTORC1 signaling pathway.

Gene Set Enrichment Analysis revealed that the mTORC1 and KRAS signaling pathways were downregulated in the infarcted Cilp1 KO hearts compared to WT hearts (Online Figure VIA). The mTORC1/S6 signaling pathway is known to regulate protein synthesis, cell growth, and proliferation in response to growth conditions. The EGFR/KRAS signaling activates mTORC1 via the MAP Kinase Erk [39]. Western blot analysis confirmed that the mTORC1/S6 signaling was upregulated in the IA of WT hearts and significantly attenuated in the KO hearts (Figure 6A). Immunofluorescent images co-stained with pS6 and αSMA indicated that the majority of the pS6 signals were from the myofibroblast (Figure 6B).

NRV cFbs undergo spontaneous myofibroblast differentiation and express aSMA when cultured in plastic plates[40, 41]. We treated NRV cFbs with condition medium from HEK293 cells transfected with control vector, NCilp1, or signal sequence deleted NCilp1/ΔSS, and with recombinant human CILP1 protein and investigated their effect on downstream signaling pathways, global protein synthesis, and cell proliferation. CILP1 activated

the mTORC1, MAPK, and Akt signaling (Figure 6C). NCilp1-conditioned medium or recombinant CILP1 protein increased global protein synthesis in NRV cFbs compared to control or NCilp1/ΔSS-condition medium treated cells as assayed by puromycin incorporation assays [42] (Figure 6D). NRV cFbs treated with NCilp1-conditioned medium or CILP1 also showed significantly increased proliferation as assayed by BrdU-pulse labeling experiments (Figure 6E) and CCK8 kits (Online Figure VIB). CILP1-stimulated cell proliferation was inhibited significantly by mTOR inhibitor rapamycin and to a lesser extent by MAPK inhibitor PD98059 (Figure 6E), indicating that Cilp1 promoted myofibroblast proliferation mainly via the mTOR signaling pathway and perhaps partially via the MAPK pathway. We also knocked down (KD) Cilp1 in NRV cFbs using Cilp1 specific siRNA. Cilp1 KD resulted in downregulation of expression of cell cycle genes such as Aurka/b, Ccna2 and Mcm3 and αSMA (Figure 6F) and reduced cell proliferation (Figure 6G). Recombinant CILP1 also promoted proliferation of adult cFbs (Figure 6H). *Cilp1* KD in adult cFbs resulted in downregulation of expression of cell cycle genes (Figure 6I).

Cilp1 regulates collagen remodeling.

We tested the effect of *Cilp1*-deletion on the collagen remodeling in the infarcted heart. Deletion of *Cilp1* resulted in an attenuated expression of collagens (Col1A1, Col3A1, and Col5A1) and fibrosis-related genes such as FN, Postn, and αSMA in the IA at post-MI day 7 compared to WT hearts (Figure 7A). Interestingly, behaving differently from the IA, the expression of Col3A1 and Postn in the sham *Cilp1* KO hearts were higher than those of WT hearts. Biaxial mechanical behavior of left ventricle showed that *Cilp1* KO hearts at baseline had a stiffer mechanical curve in the longitudinal direction than WT hearts although it's not statistically significant (Figure 7B, KO sham vs WT sham), consistent with higher Col3A1 expression in the KO hearts. While MI-injury led to a significant increase in circumferential stiffening in WT hearts, it had little effect on the KO hearts (Figure 7B WT MI vs KO MI). This could be explained by significantly increased amounts of fibroblasts, thus increased production of collagen in infarcted WT hearts compared to KO hearts. We also stained collagens of infarcted WT and KO hearts with picrosirius red (PSR) to assess the organization of the collagen fibers. WT hearts had dense green/yellowish color in birefringent image, a characteristic of thicker, more mature collagen fiber (Figure 7C). In contrast, *Cilp1* KO hearts showed a mostly green birefringence pattern of immature collagen that had greater space between them (Figure 7C). *Cilp1* KO mice have no overt cardiac phenotype at baseline. That being said, the difference of Col3A1 and Postn expression between KO and WT heart at baseline suggested that it is possible that Cilp1 inactivation may result in alteration in some of ECM gene expression and/or cellular composition of the hear ECM at baseline.

Overexpression of NCilp1 in myofibroblasts promotes adverse post-MI cardiac remodeling.

To test whether overexpression of Cilp1 in myofibroblasts can promote cell proliferation and adverse post-MI remodeling in vivo, we generated transgenic mice that express C-terminal GFP tagged NCilp1 in myofibroblasts driven by the Periostin(Postn) promoter plus 304bp enhancer [43, 44] (Figure 8A). It has been shown that existing resident fibroblast population contributes to the majority of collagen-producing myofibroblasts that are uniquely labeled by Periostin whereas other cell types such as endothelial cells, pericytes, and immune

cells contribute little [3, 45]. We established two transgenic lines with Cilp1 expression level comparable to the endogenous protein in the infarcted heart (Figure 8A, lower panel). No NCilp1-GFP cells were observed in Tg hearts at baseline/sham hearts whereas expression of NCilp1-GFP in myofibroblasts was confirmed by GFP co-stained with vimentin and aSMA in infarcted hearts after injury (Online Figure VIIA-B). No GFP staining was observe in $CD31^+$ cells (Online Figure VIIC). Overexpression of NCilp1 in myofibroblasts resulted in exacerbated adverse post-MI remodeling with reduced cardiac function (Figure 8B). LVESD was significantly increased in Tg mouse hearts compared to WT hearts (Figure 8C, left panel). Although LVEDD of Tg hearts were increased, they were not statistically significant (Figure 8C, right panel). NCilp1-Tg mice also had increased HW/BW (Figure 8D), lung weight (LW)/BW (Figure 8E), and infarct size (Figure 8F-G) compared to WT littermates. We noticed that WT littermates from Cilp1-Tg mouse cohort had different post-MI response from WT littermates from Cilp1 KO mouse cohort, they had smaller FS at post-MI day7, which is likely due to the strain difference [46, 47]. Consistent with worsened post-MI remodeling, ECM fibrosis-related genes were also upregulated in infarcted Tg hearts over WT hearts (Figure 8H-J). Overexpression of Cilp1 in myofibroblasts resulted in significantly increased number of αSMA^+ myofibroblasts in the IA of post-MI day 7 Tg-hearts compared to WT littermates (Figure 8K). BrdU proliferation assays indicated increased myofibroblast proliferation in NCilp1-Tg hearts at post-MI day 3 (Figure 8L) and increased $vimentin^+$ cells at post-MI day 7 compared to WT hearts (Figure 8M). Western blot analysis indicated that infarcted Tg hearts had increased pS6 and reduced pSmad3 compared to WT hearts (Figure 8N). Comparing changes in Akt and MAPK signaling in infarcted Cilp1 KO hearts over WT littermates (Figure 6A), changes in pAkt and pErk in infarcted Tg hearts over WT controls (Figure 8N) were much smaller, suggesting that Cilp1 in cell types other than the fibroblast may contribute to post-MI Akt and MAPK signaling.

DISCUSSION

In this study we investigated the role of Cilp1 in pathological cardiac remodeling and myocardial fibrosis. Prior studies indicated that Cilp1 was upregulated in diseased human heart tissues and in pathological remodeling mouse hearts [19, 20, 23]. However, whether Cilp1 can be used as a biomarker and its role in pathological cardiac remodeling remain elusive. Cilp1 was shown upregulated in heart tissues but paradoxically downregulated in the serum of heart failure patients [23]. We and others showed that Cilp1 was expressed predominantly in cardiac fibroblasts. Nonetheless, Li and co-workers suggested that Cilp1 was expressed in cardiomyocytes and observed that Cilp1 knockdown in cardiomyocytes enhanced pathological cardiac remodeling after TAC injury, suggesting that Cilp1 may play a protective role against adverse cardiac remodeling and fibrosis [20].

Our studies indicated that Cilp1 promoted pathological cardiac remodeling in response to TAC and MI injury. Cilp1 was upregulated in TAC- and MI-injured hearts (Figures 1 & 2). The upregulation of Cilp1 in the remodeling heart can be attenuated by inhibitors of cardiac fibrosis (Figure 2B). Contrary to a prior study showing Cilp1 was downregulated in blood of heart failure patients [23], our studies revealed that Cilp1 was upregulated (Figure 2F). The inconsistence between the two studies may be due to the anti-Cilp1 antibodies that were derived against different parts of the protein. Cilp1 is cleaved at amino acid 721

upon secretion. There are likely three forms of the protein in the circulation: full-length protein and cleaved N- and C-terminal fragments. The anti-Cilp1 antibody used in our study is derived against N-terminal part of the protein (NCilp1) and thus is able to capture both NCilp1 and full-length Cilp1. On the other hand, the antibody used in Park et al.'s study (Biomatik CAU24346) is derived against middle part of Cilp1 (amino acid 603–846). Only full-length Cilp1 was captured [23]. Although the relative amount of full-length Cilp1 and its cleaved fragments in the circulation remains to be determined, the full-length protein is likely to be lower than that of cleaved fragments. As our study indicated that the pathological activity of Cilp1 is within its N-terminal part and NCilp1 was upregulated in both the diseased heart and blood, we conclude that NCilp1 may be a better biomarker/theranostic marker for pathological remodeling and myocardial fibrosis. The discrepancy between the two studies may also be due to the sample size. The cohort in our study contained 37 normal healthy controls and 57 DCM patients whereas the one in Park et al 's study had 23 normal healthy controls and 22 heart failure patients.

Our loss-functional studies of Cilp1 with *Cilp1* KO mice indicate that *Cilp1*-deletion resulted in attenuated post-MI cardiac remodeling with better cardiac function and reduced fibrosis compared to WT littermates (Figure 3). *Cilp1* KO hearts had reduced number of immune cells and inflammatory gene expression, reduced myofibroblasts, and enhanced microvasculature survival compared to WT controls (Figure 4). Conversely, overexpression of Cilp1 in myofibroblasts resulted in exacerbated post-MI remodeling with decreased cardiac function and increased infarct size (Figure 8). These results thus provide strong support for a pathological role of Cilp1 in driving adverse post-MI remodeling and myocardial fibrosis. Consistent with its role in promoting adverse post-MI cardiac remodeling, we showed that Cilp1 played a similar role in promoting TAC-induced hypertrophic remodeling (Figure 3). Our results contradict to that of a prior report showing Cilp1 inhibiting post-TAC hypertrophic remodeling [20]. The conclusion from Zhang et al's study [20] was based on the post-TAC cardiac phenotypes of knockdown and overexpressing Cilp1 in cardiomyocytes without considering the contribution of fibroblast Cilp1, thus casting doubts on the relevance of the conclusion.

Mechanistically, Cilp1 may promote adverse cardiac remodeling and myocardial fibrosis by promoting myofibroblast proliferation via the mTOR pathway. This is supported by the following evidences: 1) deletion of *Cilp1* in mice resulted in an attenuated post-MI remodeling and decreased myofibroblast proliferation (Figures 3A-E, 4C, & 5E); whereas 2) overexpression of Cilp1 in myofibroblasts promoted cell proliferation and worsened adverse cardiac remodeling (Figure 8); 3) secreted NCilp1 protein in conditioned medium or recombinant CILP1 protein activated the mTORC1 signaling pathway and promoted myofibroblast proliferation (Figure 6C-E); 4) the mTORC1 signaling was upregulated in the myofibroblast of WT IA and attenuated in *Cilp1* KO IA (Figure 6A-B); 5) inhibition of mTOR abolished Cilp1-promoted myofibroblast proliferation (Figure 6E); and 5) Cilp1 KD in myofibroblasts downregulated cell cycle gene expression (Figure 6F & 6I) and cell proliferation (Figure 6G). The MAPK pathway may be involved in Cilp1-regulated cell proliferation as well since it can be activated by Cilp1 and inhibition of ERK by PD98059 downregulated Cilp1-promoted myofibroblast proliferation even though the downregulation was only partial (Figure 6E).

There are several shortcomings for using immunofluorescence staining to study myofibroblast proliferation in vivo. First, there is no unique marker for labeling myofibroblasts; aSMA also stains smooth muscle cells around vasculature and vimentin stains endothelial cells as well. Second, myofibroblast morphology can range from circular (like vessels) to long spindles depending on their spatial locations. Immunofluorescence staining cannot determine the cell type based on their morphology. Despite these caveats, the following arguments support our conclusion that Cipl1 promotes myofibroblast proliferation. First, microvasculature stained by CD31 were similar between post-MI day 3 and day 7 in KO hearts (Figure 4D), therefore the downregulation of $aSMA^+$ cells in infarcted KO hearts compared to WT hearts cannot come from smooth muscle cells around vessels. The difference of myofibroblast proliferation between WT and KO hearts based on aSMA staining could be underestimated in our analysis. Second, experiments using both markers (aSMA and vimentin) yielded similar conclusion. Most importantly, recombinant protein or Cilp1-conditioned medium can promote proliferation of NRV and adult cFbs in vitro. Other things that are worth mentioning and require further investigations, including 1) Cilp1 may have pro-proliferative function for other heart cell types as well since it is a secreted protein; 2) Cilp1 from other heart cell types or organs may contribute to post-MI cardiac remodeling since it is in the circulating blood and our studies are based on global *Cilp1*-deletion; 3) the mechanism by which Cip1 promotes activation of the mTOR signaling remains to be determined and may involve a receptor mediated signaling pathway.

Cilp1 is known to inhibit Tgfβ-induced myofibroblast differentiation and collagen production [18, 19, 21]. Consistently, we observed upregulation of Col3A1 and Postn in *Cilp1* KO hearts under baseline physiological condition (Figure 7A). We also noticed that although aSMA was downregulated in *Cilp1* KD cFbs compared to control KD cells (Figure 6F & 6I), it was similar in post-MI day 3 between *Cilp1* KO and WT hearts (Fig. 4C). The apparent discrepancy between in vitro and in vivo may be explained by the fact that loss of *Cilp1* in vivo may result in upregulation of Tgfβ signaling (Figure 6A) which can promote aSMA expression in a feed-back loop mechanism. The consequence of the anti-Tgfβ activity of Cilp1 on collagen expression is opposite from its action on promoting myofibroblast proliferation, suggesting that the anti-Tgfβ and pro-proliferation activities of Cilp1 may be context dependent. Activation of Tgfβ/Smad3 in activated fibroblasts has been shown to downregulate matrix metalloproteinase (MMP)-mediated matrix degradation and protect mice against TAC-induced heart remodeling [5]. Cilp1 may promote pathological cardiac remodeling via MMP-associated function of Tgfb in myofibroblast rather than the pro-fibrotic function of Tgfb. Future studies using mouse model where *Cilp1* can be conditionally deleted specifically in cardiac fibroblast and at various post-MI time points are needed to test this hypothesis.

We attempted to use recombinant CILP1 protein to rescue downregulated cell cycle gene expression in Cilp1 KD cFbs and observed no rescue. We found that Cilp1 may interact with nuclear protein NEDD1 and CDC20 (URL: https://thebiogrid.org/114057/summary/homo-sapiens/cilp.html), suggesting that Cilp1 may have fibroblast cell autonomous function that is different from its role as a paracrine factor. Studies using mouse with Cilp1-deleted specifically in cardiac fibroblasts is warranted in the future to test this hypothesis.

In summary, we have identified a novel function of Cilp1 in promoting pathological cardiac remodeling upon injury. Our studies suggest that Cilp1 may serve as a potential biomarker for adverse remodeling and promote myofibroblast proliferation and myocardial fibrosis during the pathological remodeling. Matricellular proteins are clinically attractive targets owing to their accessibility to systemically delivered therapeutic reagents. Our mechanistic studies established Cilp1 as a target for pathological cardiac remodeling and myocardial fibrosis and inhibition of the cellular function of Cilp1 may provide a therapeutic strategy in blocking progression of heart failure.

Supplementary Material

Refer to Web version on PubMed Central for supplementary material.

ACKNOWLEDGMENTS

We thank Ms Alicia Rizo-Liu for the assistance of making Graphic Abstract created with BioRender.com.

SOURCE OF FUNDING

This work is supported in part by grants from National Institute of Health (NIH) (HL109471 and CA215063 to ZPL; HL128215, HL126012, and HL147933 to JAH; GM111295 to QSZ), and American Heart Associate (AHA) 19TP34910172 to ZPL.

Nonstandard Abbreviations and Acronyms:

αSMA	smooth muscle alpha-actin
BAPN	β-aminopropionitrile
Cilp1	Cartilage intermediate layer protein 1
DCM	Dilated cardiomyopathy
ECM	Extracellular matrix
HCM	Hypertrophic cardiomyopathy
IA	Infarct area
KO	Knock out
MI	Myocardial infarction
NPP	Nucleotide pyrophosphatase phosphodiesterase
RA	Remote area
Tg	Transgenic
TSR	Thrombospondin type 1 repeat domain
TAC	Trans aortic constriction
WT	Wild type

REFERENCES

1. Azevedo PS, Polegato BF, Minicucci MF, Paiva SA, Zornoff LA. Cardiac remodeling: Concepts, clinical impact, pathophysiological mechanisms and pharmacologic treatment. Arq Bras Cardiol. 2016;106:62–69 [PubMed: 26647721]
2. Burchfield JS, Xie M, Hill JA. Pathological ventricular remodeling: Mechanisms: Part 1 of 2. Circulation. 2013;128:388–400 [PubMed: 23877061]
3. Tallquist MD. Cardiac fibroblast diversity. Annu Rev Physiol. 2020;82:63–78 [PubMed: 32040933]
4. Park S, Nguyen NB, Pezhouman A, Ardehali R. Cardiac fibrosis: Potential therapeutic targets. Transl Res. 2019;209:121–137 [PubMed: 30930180]
5. Russo I, Cavalera M, Huang S, Su Y, Hanna A, Chen B, Shinde AV, Conway SJ, Graff J, Frangogiannis NG. Protective effects of activated myofibroblasts in the pressure-overloaded myocardium are mediated through smad-dependent activation of a matrix-preserving program. Circ Res. 2019;124:1214–1227 [PubMed: 30686120]
6. Wintrich J, Kindermann I, Ukena C, Selejan S, Werner C, Maack C, Laufs U, Tschope C, Anker SD, Lam CSP, Voors AA, Bohm M. Therapeutic approaches in heart failure with preserved ejection fraction: Past, present, and future. Clin Res Cardiol. 2020;109:1079–1098 [PubMed: 32236720]
7. Parichatikanond W, Luangmonkong T, Mangmool S, Kurose H. Therapeutic targets for the treatment of cardiac fibrosis and cancer: Focusing on tgf-beta signaling. Front Cardiovasc Med. 2020;7:34 [PubMed: 32211422]
8. Hinderer S, Schenke-Layland K. Cardiac fibrosis - a short review of causes and therapeutic strategies. Adv Drug Deliv Rev. 2019;146:77–82 [PubMed: 31158407]
9. Vagnozzi RJ, Maillet M, Sargent MA, Khalil H, Johansen AKZ, Schwanekamp JA, York AJ, Huang V, Nahrendorf M, Sadayappan S, Molkentin JD. An acute immune response underlies the benefit of cardiac stem cell therapy. Nature. 2020;577:405–409 [PubMed: 31775156]
10. Aghajanian H, Kimura T, Rurik JG, Hancock AS, Leibowitz MS, Li L, Scholler J, Monslow J, Lo A, Han W, Wang T, Bedi K, Morley MP, Linares Saldana RA, Bolar NA, McDaid K, Assenmacher CA, Smith CL, Wirth D, June CH, Margulies KB, Jain R, Pure E, Albelda SM, Epstein JA. Targeting cardiac fibrosis with engineered t cells. Nature. 2019;573:430–433 [PubMed: 31511695]
11. de Boer RA, De Keulenaer G, Bauersachs J, Brutsaert D, Cleland JG, Diez J, Du XJ, Ford P, Heinzel FR, Lipson KE, McDonagh T, Lopez-Andres N, Lunde IG, Lyon AR, Pollesello P, Prasad SK, Tocchetti CG, Mayr M, Sluijter JPG, Thum T, Tschope C, Zannad F, Zimmermann WH, Ruschitzka F, Filippatos G, Lindsey ML, Maack C, Heymans S. Towards better definition, quantification and treatment of fibrosis in heart failure. A scientific roadmap by the committee of translational research of the heart failure association (hfa) of the european society of cardiology. Eur J Heart Fail. 2019;21:272–285 [PubMed: 30714667]
12. Lewis GA, Dodd S, Naish JH, Selvanayagam JB, Dweck MR, Miller CA. Considerations for clinical trials targeting the myocardial interstitium. JACC Cardiovasc Imaging. 2019;12:2319–2331 [PubMed: 31422145]
13. Gourdie RG, Dimmeler S, Kohl P. Novel therapeutic strategies targeting fibroblasts and fibrosis in heart disease. Nat Rev Drug Discov. 2016;15:620–638 [PubMed: 27339799]
14. Lorenzo P, Neame P, Sommarin Y, Heinegard D. Cloning and deduced amino acid sequence of a novel cartilage protein (cilp) identifies a proform including a nucleotide pyrophosphohydrolase. J Biol Chem. 1998;273:23469–23475 [PubMed: 9722584]
15. Wang Z, Kim JH, Higashino K, Kim SS, Wang S, Seki S, Hutton WC, Yoon ST. Cartilage intermediate layer protein (cilp) regulation in intervertebral discs. The effect of age, degeneration, and bone morphogenetic protein-2. Spine (Phila Pa 1976). 2012;37:E203–208 [PubMed: 21857406]
16. Johnson K, Farley D, Hu SI, Terkeltaub R. One of two chondrocyte-expressed isoforms of cartilage intermediate-layer protein functions as an insulin-like growth factor 1 antagonist. Arthritis Rheum. 2003;48:1302–1314 [PubMed: 12746903]
17. Nakamura I, Okawa A, Ikegawa S, Takaoka K, Nakamura Y. Genomic organization, mapping, and polymorphisms of the gene encoding human cartilage intermediate layer protein (cilp). J Hum Genet. 1999;44:203–205 [PubMed: 10319588]

18. Seki S, Tsumaki N, Motomura H, Nogami M, Kawaguchi Y, Hori T, Suzuki K, Yahara Y, Higashimoto M, Oya T, Ikegawa S, Kimura T. Cartilage intermediate layer protein promotes lumbar disc degeneration. Biochem Biophys Res Commun. 2014;446:876–881 [PubMed: 24631904]
19. van Nieuwenhoven FA, Munts C, Op't Veld RC, Gonzalez A, Diez J, Heymans S, Schroen B, van Bilsen M. Cartilage intermediate layer protein 1 (cilp1): A novel mediator of cardiac extracellular matrix remodelling. Sci Rep. 2017;7:16042 [PubMed: 29167509]
20. Zhang CL, Zhao Q, Liang H, Qiao X, Wang JY, Wu D, Wu LL, Li L. Cartilage intermediate layer protein-1 alleviates pressure overload-induced cardiac fibrosis via interfering tgf-beta1 signaling. J Mol Cell Cardiol. 2018;116:135–144 [PubMed: 29438665]
21. Shindo K, Asakura M, Min K_D, Ito S, Fu H-Y, Yamazaki S, Takahashi A, Imazu M, Fukuda H, Nakajima Y, Asanuma H, Minamino T, Takashima S, Minamino N, Mochizuki N, Kitakaze M. Cartilage intermediate layer protein 1 suppresses tgf-β signaling in cardiac fibroblasts. International Journal of Geronotology. 2017;11:67–74
22. Barallobre-Barreiro J, Didangelos A, Schoendube FA, Drozdov I, Yin X, Fernandez-Caggiano M, Willeit P, Puntmann VO, Aldama-Lopez G, Shah AM, Domenech N, Mayr M. Proteomics analysis of cardiac extracellular matrix remodeling in a porcine model of ischemia/reperfusion injury. Circulation. 2012;125:789–802 [PubMed: 22261194]
23. Park S, Ranjbarvaziri S, Zhao P, Ardehali R. Cardiac fibrosis is associated with decreased circulating levels of full-length cilp in heart failure. JACC Basic Transl Sci. 2020;5:432–443 [PubMed: 32478206]
24. McLellan MA, Skelly DA, Dona MSI, Squiers GT, Farrugia GE, Gaynor TL, Cohen CD, Pandey R, Diep H, Vinh A, Rosenthal NA, Pinto AR. High-resolution transcriptomic profiling of the heart during chronic stress reveals cellular drivers of cardiac fibrosis and hypertrophy. Circulation. 2020;142:1448–1463 [PubMed: 32795101]
25. Scholten D, Trebicka J, Liedtke C, Weiskirchen R. The carbon tetrachloride model in mice. Lab Anim. 2015;49:4–11 [PubMed: 25835733]
26. Walters DM, Kleeberger SR. Mouse models of bleomycin-induced pulmonary fibrosis. Curr Protoc Pharmacol. 2008;Chapter 5:Unit 5 46 [PubMed: 22294226]
27. Ho JE, Liu C, Lyass A, Courchesne P, Pencina MJ, Vasan RS, Larson MG, Levy D. Galectin-3, a marker of cardiac fibrosis, predicts incident heart failure in the community. J Am Coll Cardiol. 2012;60:1249–1256 [PubMed: 22939561]
28. Zhang QJ, Chen HZ, Wang L, Liu DP, Hill JA, Liu ZP. The histone trimethyllysine demethylase jmjd2a promotes cardiac hypertrophy in response to hypertrophic stimuli in mice. J Clin Invest. 2011;121:2447–2456 [PubMed: 21555854]
29. El Hajj EC, El Hajj MC, Ninh VK, Gardner JD. Cardioprotective effects of lysyl oxidase inhibition against volume overload-induced extracellular matrix remodeling. Exp Biol Med (Maywood). 2016;241:539–549 [PubMed: 26582054]
30. Gonzalez-Santamaria J, Villalba M, Busnadiego O, Lopez-Olaneta MM, Sandoval P, Snabel J, Lopez-Cabrera M, Erler JT, Hanemaaijer R, Lara-Pezzi E, Rodriguez-Pascual F. Matrix cross-linking lysyl oxidases are induced in response to myocardial infarction and promote cardiac dysfunction. Cardiovasc Res. 2016;109:67–78 [PubMed: 26260798]
31. Rosin NL, Sopel MJ, Falkenham A, Lee TD, Legare JF. Disruption of collagen homeostasis can reverse established age-related myocardial fibrosis. Am J Pathol. 2015;185:631–642 [PubMed: 25701883]
32. Satija R, Farrell JA, Gennert D, Schier AF, Regev A. Spatial reconstruction of single-cell gene expression data. Nat Biotechnol. 2015;33:495–502 [PubMed: 25867923]
33. Tabula Muris C, Overall c, Logistical c, Organ c, processing, Library p, sequencing, Computational data a, Cell type a, Writing g, Supplemental text writing g, Principal i. Single-cell transcriptomics of 20 mouse organs creates a tabula muris. Nature. 2018;562:367–372 [PubMed: 30283141]
34. Skelly DA, Squiers GT, McLellan MA, Bolisetty MT, Robson P, Rosenthal NA, Pinto AR. Single-cell transcriptional profiling reveals cellular diversity and intercommunication in the mouse heart. Cell Rep. 2018;22:600–610 [PubMed: 29346760]

35. Schafer S, Viswanathan S, Widjaja AA, Lim WW, Moreno-Moral A, DeLaughter DM, Ng B, Patone G, Chow K, Khin E, Tan J, Chothani SP, Ye L, Rackham OJL, Ko NSJ, Sahib NE, Pua CJ, Zhen NTG, Xie C, Wang M, Maatz H, Lim S, Saar K, Blachut S, Petretto E, Schmidt S, Putoczki T, Guimaraes-Camboa N, Wakimoto H, van Heesch S, Sigmundsson K, Lim SL, Soon JL, Chao VTT, Chua YL, Tan TE, Evans SM, Loh YJ, Jamal MH, Ong KK, Chua KC, Ong BH, Chakaramakkil MJ, Seidman JG, Seidman CE, Hubner N, Sin KYK, Cook SA. Il-11 is a crucial determinant of cardiovascular fibrosis. Nature. 2017;552:110–115 [PubMed: 29160304]
36. Schmitt JP, Kamisago M, Asahi M, Li GH, Ahmad F, Mende U, Kranias EG, MacLennan DH, Seidman JG, Seidman CE. Dilated cardiomyopathy and heart failure caused by a mutation in phospholamban. Science. 2003;299:1410–1413 [PubMed: 12610310]
37. Frangogiannis NG. The extracellular matrix in myocardial injury, repair, and remodeling. J Clin Invest. 2017;127:1600–1612 [PubMed: 28459429]
38. Fu X, Khalil H, Kanisicak O, Boyer JG, Vagnozzi RJ, Maliken BD, Sargent MA, Prasad V, Valiente-Alandi I, Blaxall BC, Molkentin JD. Specialized fibroblast differentiated states underlie scar formation in the infarcted mouse heart. J Clin Invest. 2018;128:2127–2143 [PubMed: 29664017]
39. Saxton RA, Sabatini DM. Mtor signaling in growth, metabolism, and disease. Cell. 2017;169:361–371
40. Santiago JJ, Dangerfield AL, Rattan SG, Bathe KL, Cunnington RH, Raizman JE, Bedosky KM, Freed DH, Kardami E, Dixon IM. Cardiac fibroblast to myofibroblast differentiation in vivo and in vitro: Expression of focal adhesion components in neonatal and adult rat ventricular myofibroblasts. Dev Dyn. 2010;239:1573–1584 [PubMed: 20503355]
41. Tarbit E, Singh I, Peart JN, Rose'Meyer RB. Biomarkers for the identification of cardiac fibroblast and myofibroblast cells. Heart Fail Rev. 2019;24:1–15 [PubMed: 29987445]
42. Aviner R. The science of puromycin: From studies of ribosome function to applications in biotechnology. Comput Struct Biotechnol J. 2020;18:1074–1083 [PubMed: 32435426]
43. Lindsley A, Snider P, Zhou H, Rogers R, Wang J, Olaopa M, Kruzynska-Frejtag A, Koushik SV, Lilly B, Burch JB, Firulli AB, Conway SJ. Identification and characterization of a novel schwann and outflow tract endocardial cushion lineage-restricted periostin enhancer. Dev Biol. 2007;307:340–355 [PubMed: 17540359]
44. Zhang J, Tao R, Campbell KF, Carvalho JL, Ruiz EC, Kim GC, Schmuck EG, Raval AN, da Rocha AM, Herron TJ, Jalife J, Thomson JA, Kamp TJ. Functional cardiac fibroblasts derived from human pluripotent stem cells via second heart field progenitors. Nat Commun. 2019;10:2238 [PubMed: 31110246]
45. Kanisicak O, Khalil H, Ivey MJ, Karch J, Maliken BD, Correll RN, Brody MJ, SC JL, Aronow BJ, Tallquist MD, Molkentin JD. Genetic lineage tracing defines myofibroblast origin and function in the injured heart. Nat Commun. 2016;7:12260 [PubMed: 27447449]
46. van den Borne SW, van de Schans VA, Strzelecka AE, Vervoort-Peters HT, Lijnen PM, Cleutjens JP, Smits JF, Daemen MJ, Janssen BJ, Blankesteijn WM. Mouse strain determines the outcome of wound healing after myocardial infarction. Cardiovasc Res. 2009;84:273–282 [PubMed: 19542177]
47. Lusis AJ, Seldin MM, Allayee H, Bennett BJ, Civelek M, Davis RC, Eskin E, Farber CR, Hui S, Mehrabian M, Norheim F, Pan C, Parks B, Rau CD, Smith DJ, Vallim T, Wang Y, Wang J. The hybrid mouse diversity panel: A resource for systems genetics analyses of metabolic and cardiovascular traits. J Lipid Res. 2016;57:925–942 [PubMed: 27099397]
48. Zhu M, Goetsch SC, Wang Z, Luo R, Hill JA, Schneider J, Morris SM Jr., Liu ZP. Foxo4 promotes early inflammatory response upon myocardial infarction via endothelial arg1. Circ Res. 2015;117:967–977 [PubMed: 26438688]
49. Zhao X, Huffman KE, Fujimoto J, Canales JR, Girard L, Nie G, Heymach JV, Wistuba II, Minna JD, Yu Y. Quantitative proteomic analysis of optimal cutting temperature (oct) embedded core-needle biopsy of lung cancer. J Am Soc Mass Spectrom. 2017;28:2078–2089 [PubMed: 28752479]
50. Hu R, Huffman KE, Chu M, Zhang Y, Minna JD, Yu Y. Quantitative secretomic analysis identifies extracellular protein factors that modulate the metastatic phenotype of non-small cell lung cancer. J Proteome Res. 2016;15:477–486 [PubMed: 26736068]

51. Wang J, Zhang Y, Yu Y. Crescendo: A protein sequence database search engine for tandem mass spectra. J Am Soc Mass Spectrom. 2015;26:1077–1084 [PubMed: 25895889]

52. Zhang Y, Wang J, Ding M, Yu Y. Site-specific characterization of the asp- and glu-adp-ribosylated proteome. Nat Methods. 2013;10:981–984 [PubMed: 23955771]

53. Butler A, Hoffman P, Smibert P, Papalexi E, Satija R. Integrating single-cell transcriptomic data across different conditions, technologies, and species. Nat Biotechnol. 2018;36:411–420 [PubMed: 29608179]

54. Chen J, Bardes EE, Aronow BJ, Jegga AG. Toppgene suite for gene list enrichment analysis and candidate gene prioritization. Nucleic Acids Res. 2009;37:W305–311 [PubMed: 19465376]

55. Liu ZP, Olson EN. Suppression of proliferation and cardiomyocyte hypertrophy by champ, a cardiac-specific rna helicase. Proc Natl Acad Sci U S A. 2002;99:2043–2048 [PubMed: 11854500]

56. Melzer M, Beier D, Young PP, Saraswati S. Isolation and characterization of adult cardiac fibroblasts and myofibroblasts. J Vis Exp. 2020

NOVELTY AND SIGNIFICANCE

What Is Known?

- Cartilage intermediate layer protein 1 (Cilp1) is a matricellular protein, originally found secreted predominantly from chondrocytes in articular cartilage, that is implicated in common musculoskeletal disorders.
- Expression of Cilp1 is elevated in diseased human heart and in mouse hearts undergoing pathological cardiac remodeling induced by myocardial infarction (MI), transverse aortic constriction and angiotensin II treatment.
- Cilp1 binds transforming growth factor-β (TGF-β) and inhibits TGF-β-induced expression of collagens and α-Smooth Muscle Actin (aSMA) *in vitro*.

What New Information Does This Article Provide?

- Cilp1 was expressed predominantly in cardiac fibroblasts and upregulated in the blood of human heart failure patients.
- Deletion of *Cilp1* in mice attenuated adverse cardiac remodeling whereas overexpression of N-terminal half of the Cilp1 protein (NCilp1) in cardiac fibroblasts resulted in exacerbated post-MI remodeling.
- The mTORC1 signaling pathway was upregulated in proliferating myofibroblasts of infarcted hearts in response to MI, which was attenuated in infarcted *Cilp1* KO- compared to WT hearts.
- Recombinant CILP1 protein or conditional medium containing secreted NCilp1 promoted proliferation of cardiac fibroblasts *in vitro* via the mTORC1 signaling pathway.

Prior studies indicated that Cilp1 was upregulated in diseased human and mouse hearts. However, whether Cilp1 can be used as a biomarker, and whether it plays a role in pathological cardiac remodeling, remains elusive. Cilp1 binds transforming growth factor-β (TGF-β) and inhibits its biological function. Upregulation of Cilp1 in response to cardiac injury was thought to protect mice against stress-induced pathological remodeling and myocardial fibrosis due to the pro-fibrotic function of TGF-β. Based on gain- and loss-functional studies with Cilp1, we demonstrated that Cilp1 promoted post-MI cardiac remodeling and myocardial fibrosis. Mechanistically, we identified a novel function of Cilp1, which promotes post-MI myofibroblast proliferation via the mTORC1 signaling pathway. Our studies also showed that Cilp1 is upregulated in the blood of patients with dilated cardiomyopathy and may serve as a potential biomarker for adverse remodeling and heart failure. Matricellular proteins are clinically attractive targets owing to their accessibility to systemically delivered therapeutic reagents. Our mechanistic studies established Cilp1 as a target for pathological cardiac remodeling and myocardial fibrosis, and inhibition of the cellular function of Cilp1 may provide a therapeutic strategy to block progression of heart failure.

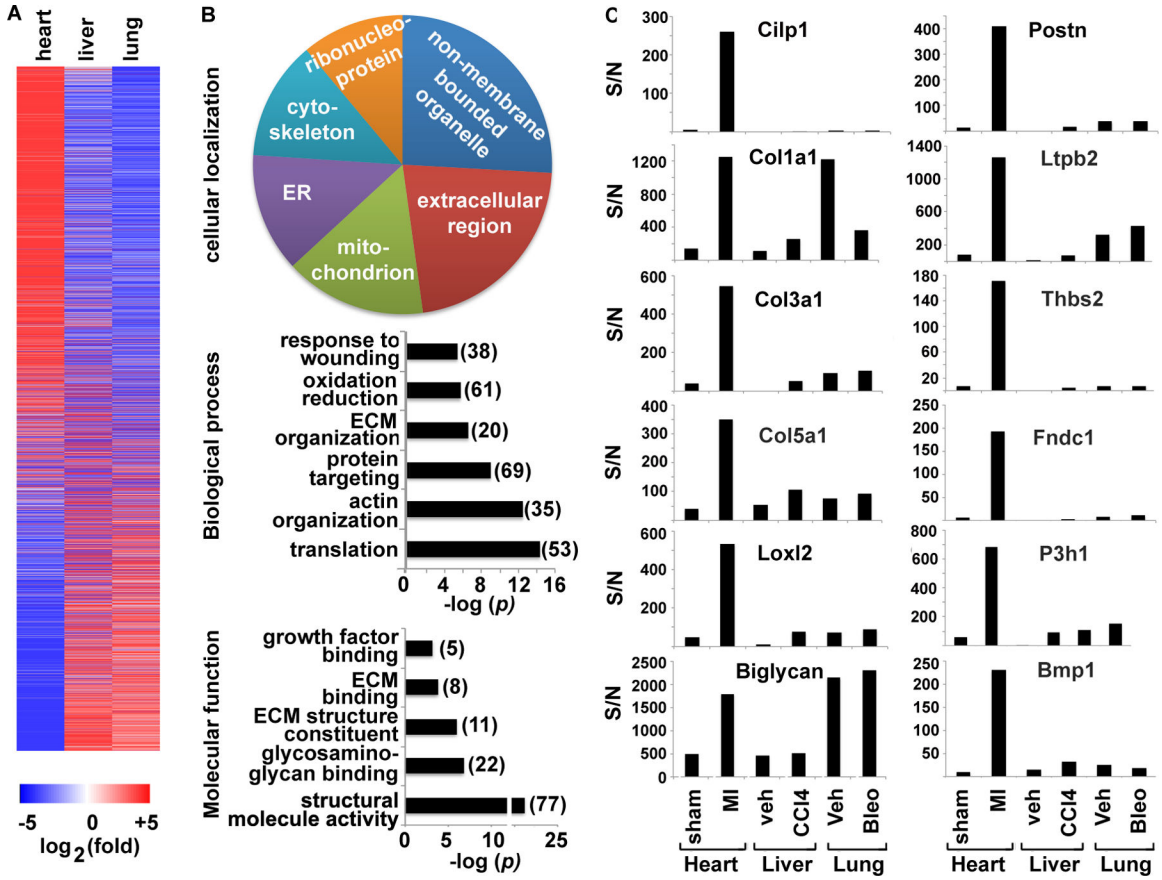

Figure 1. Comparative proteomics of mouse heart, liver and lung revealed that Cilp1 is upregulated in post-MI heart.

C57BL/6J mice were subjected to MI or CCl_4-treatment for 7 days, or Bleomycin for 14 days. Myocardial and liver fibrosis were confirmed by Trichrome blue staining. No lung fibrosis and only inflammation was observed under our current treatment protocol. Six tissue samples pooled from three individual mice were labeled with TMTsixplex and subjected to LC-MS/MS spectrometry. (A) Heat map showing fold change of MI or drug-treated tissue over sham or vehicle-treated tissue. (B) GO analysis of proteins with >=2-fold changes in the infarcted hearts. (C) Relative protein levels measured as S/N (signal/noise ratio) by mass-spectrometry of representative genes from tissues of sham/vehicle and MI/drug-treated animals.

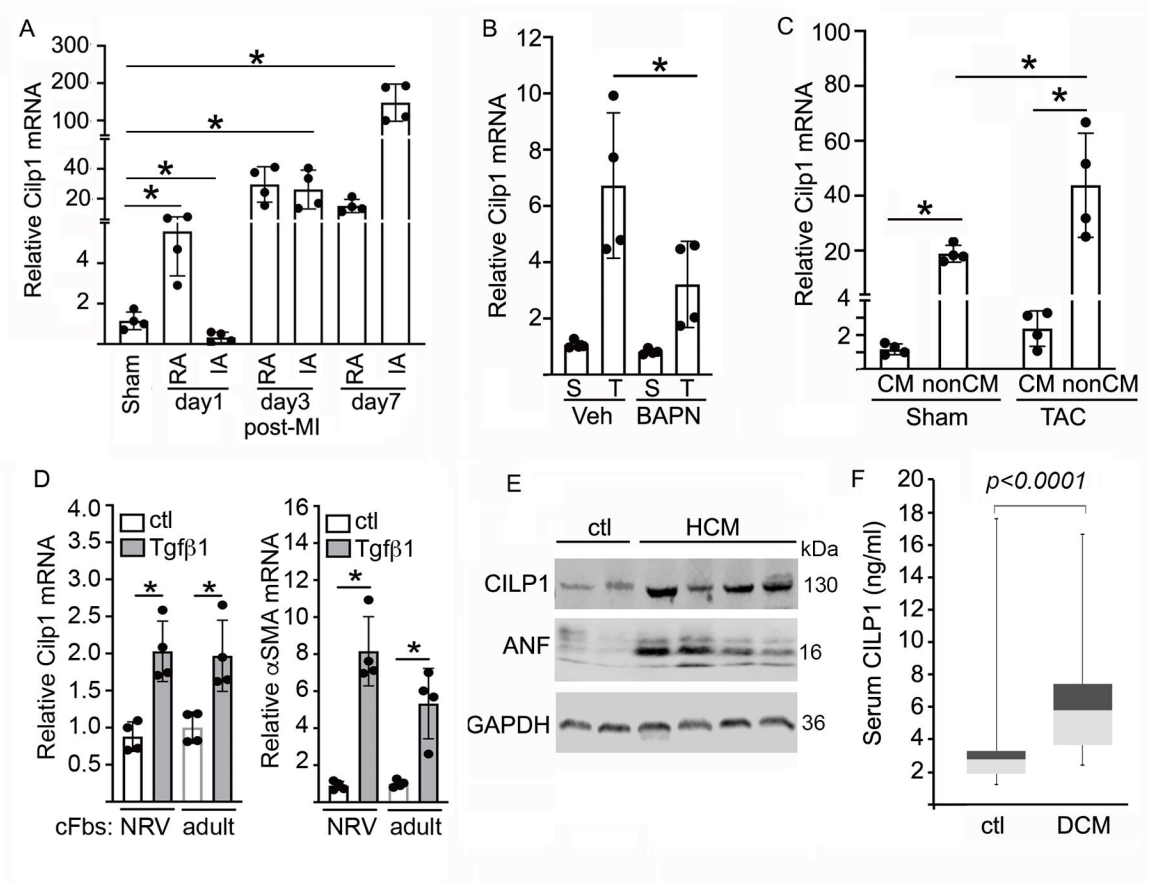

Figure 2. Cilp1 is upregulated in pathological remodeling hearts and serum of heart failure patients.

(A) Relative Cilp1 mRNA in sham and post-MI mouse hearts. (B) Relative Cilp1 mRNA in sham (S) and TAC (T) mouse hearts treated with vehicle (veh) and BAPN. (C) Relative Cilp1 mRNA in cardiomyocyte (CM) and non-cardiomyocyte (nonCM) of mouse hearts after 3 weeks of Sham and TAC surgery. (D) Relative Cilp1 and αSMA mRNA in NRV and adult cFbs stimulated without or with Tgfβ1. (E) Western blot of CILP1 and ANF proteins in normal control and hypertrophic cardiomyopathy (HCM) patient hearts. GAPDH was used as loading control. (F) Serum CILP1 levels in normal (ctl, n=37) vs DCM (n=51) human patients. Error bars are SEM. (A-D). * $p<0.05$ by student t test. F, $p<0.0001$ by Mann-Whitney test.

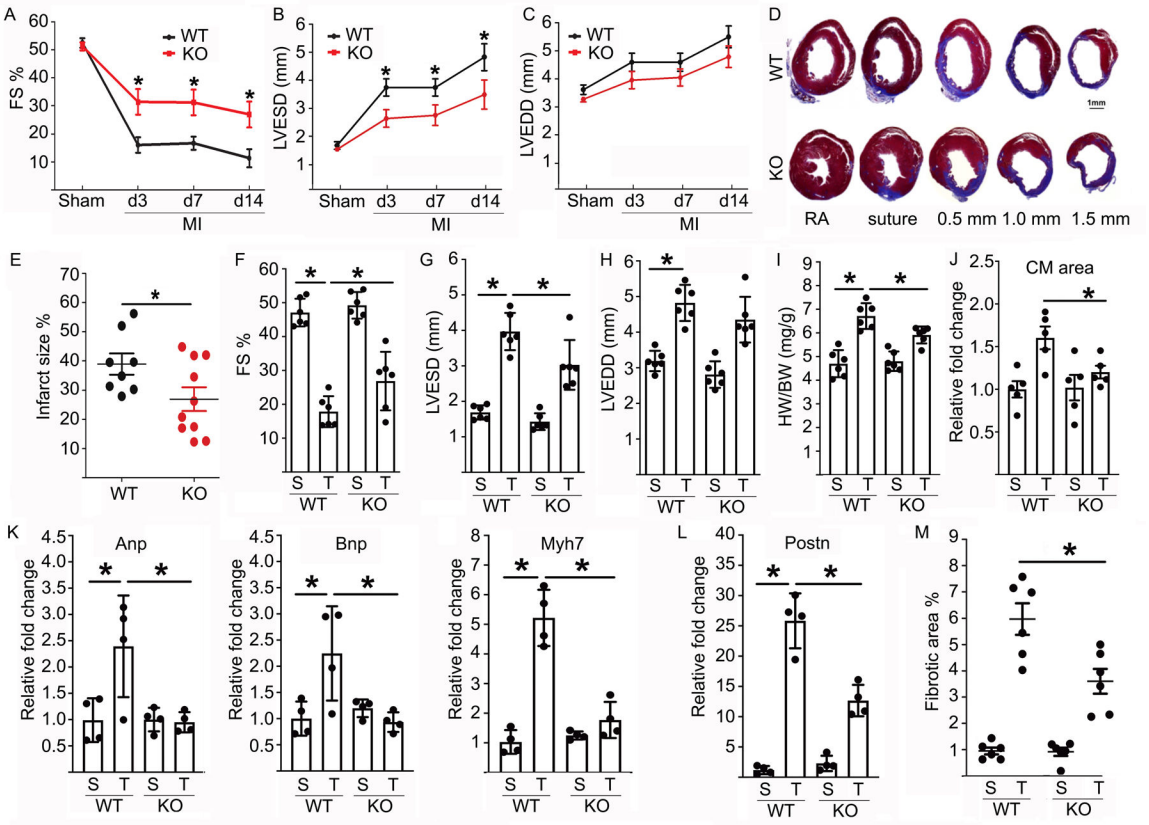

Figure 3. Cilp1-inactivation protects mice against pathological cardiac remodeling.

(A-E) *Cilp1* KO and WT mice were subjected to MI. (A) fractional shortening (FS%), (B) LVESD, and (C) LVEDD of mice at Sham and post-MI day 3, 7, & 14 (n=5–10). (D) Representative images of Masson's Trichrome-stained transverse cross sections of post-MI day 14 hearts at the levels indicated. (E) Infarct size was quantified from sections shown in D and normalized to cross-section area. (F-M) *Cilp1* KO and WT littermates were subjected to Sham (S) or TAC (T) surgery. Hearts were harvested 6 weeks later. (F) FS%, (G) LVESD, (H) LVEDD, (I) HW/BW, (J) cardiomyocyte (CM) area, (K-M) relative mRNA of fetal genes (K) and Periostin (Postn) (L) of sham and TAC WT and *Cilp1* KO mouse hearts. (M) Fibrotic area (%) of WT and *Cilp1* KO hearts after 6 weeks of sham and TAC. Error bars are SEM, * $p<0.05$ by student t test.

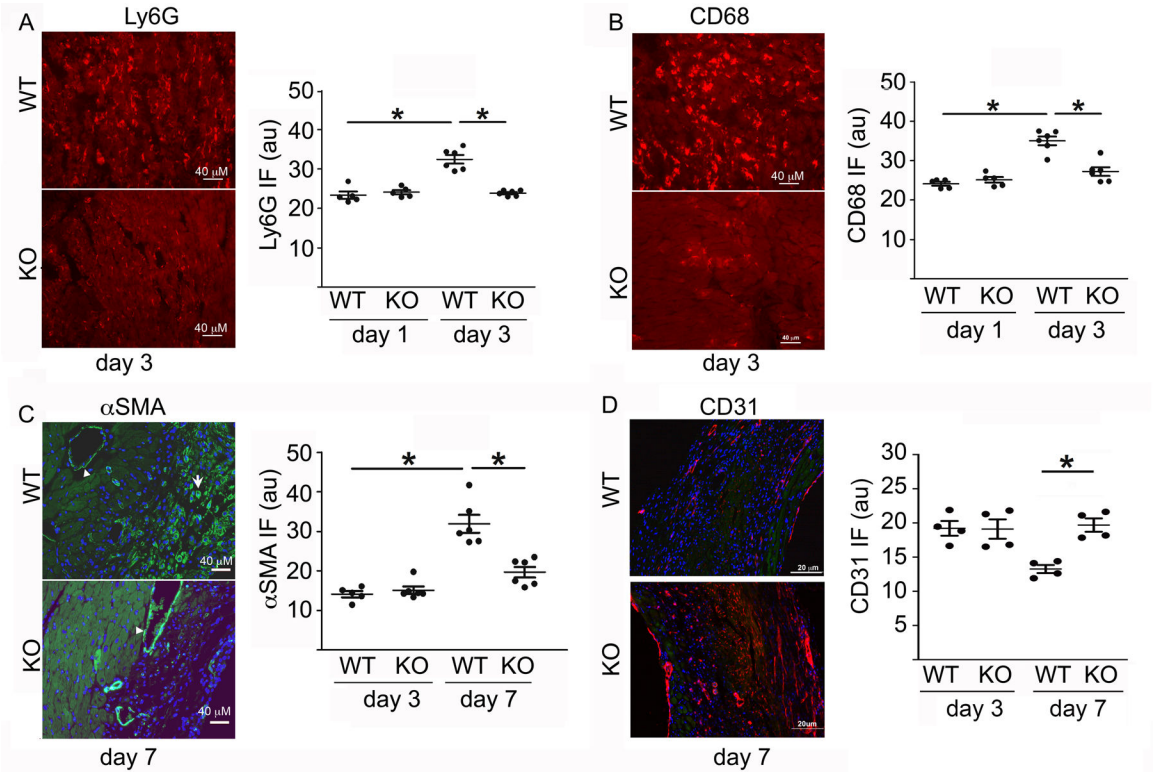

Figure 4. *Cilp1*-deletion results in reduced immune cells and myofibroblasts and enhanced microvascular survival.

(A-D, left panels) Representative micrograph of immunofluorescence staining of (A) Ly6G and (B) CD68 at post-MI day 3, (C) αSMA and (D) CD31 at post-MI day 7 of WT and *Cilp1* KO hearts. aSMA stains smooth muscle cells around vessels (arrow heads) and myofibroblasts (arrow) (C). Quantifications of relative staining of Ly6G and CD68 at post-MI day 1 and day 3, αSMA and CD31 at post-MI day 3 and day 7 are shown next to the graph. au, arbitrary unit. Error bars are SEM. * p<0.05 by student t test.

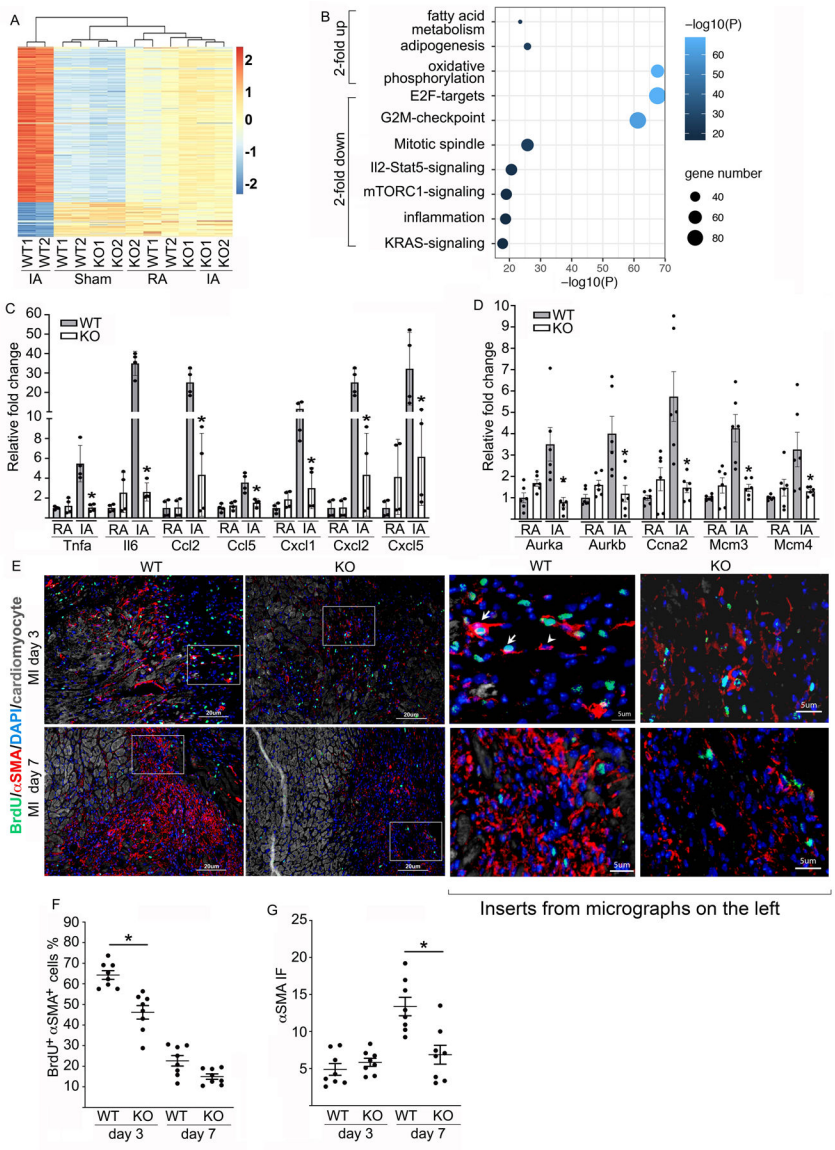

Figure 5. Cilp1 promotes post-MI inflammation and myofibroblast proliferation.

(A) Heat map of differentially expressed genes between infarcted WT and *Cilp1* KO hearts at post-MI day 3. (B) GO terms of molecular processes and signaling pathways of differentially expressed genes. (C) Relative fold change of cytokines and (D) cell cycle genes in infarcted WT and *Cilp1* KO hearts. *, KO IA vs WT IA, $p<0.05$ by student t test. (E-G) WT and *Cilp1* KO mice were pulse-labeled with BrdU (ip, 60mg/kg) for 4 hours at post-MI day 3 and day 7. Representative immunofluorescence (IF) images co-stained with antibodies against BrdU and αSMA of heart sections in the IA. Magnified inserts were shown on the right. Myofibroblasts stained with aSMA and BrdU are indicated by arrows and non-BrdU-labeled myofibroblasts is indicated by an arrowhead. Quantification of % of BrdU labeled aSMA$^+$ cells (F) and αSMA IF staining normalized to infarct area (G) at post-MI day 3 and day 7. Error bars are SEM. * $p<0.05$ by student t test.

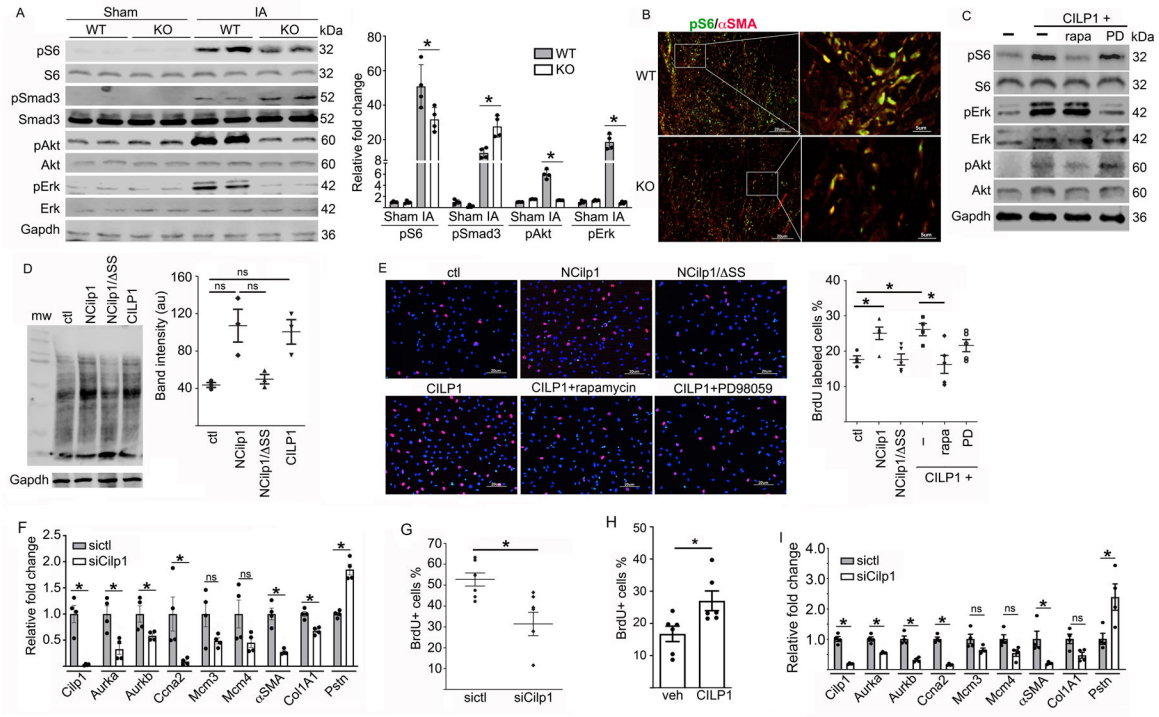

Figure 6. Cilp1 promotes myofibroblast proliferation.

(A) Representative western blot of indicted proteins from sham and IA of WT and *Cilp1* KO hearts at post-MI day 3. Quantifications were shown on the right panel (n=4). (B) Representative immunofluorescent micrographs of WT and *Cilp1* KO heart in the IA at post-MI day 3 co-stained with pS6 and αSMA. (C-E) NRV cFbs were cultured in the presence of recombinant CILP1 protein, or with condition medium from control vector, NCilp1, and NCilp1/ΔSS transfected cells, and treated with or without mTOR inhibitor rapamycin or MAPK inhibitor PD98059. (C) Western blot of cell lysates with antibodies against markers of the mTORC1 pathway (pS6), Akt pathway (pAkt), MAPK pathway (pErk), and respective loading controls. (D) NRV cFbs under indicated culture conditions were pulsed labeled with puromycin (1nM) for 15 min. Cell lysates were western blotted with antibody against puromycin (left panel) and quantified with densitometry (right panel). (E) NRV cFbs under indicated culture conditions were pulse-labeled with BrdU (10 μM) for 30min. Representative immunofluorescent images of cells co-stained with BrdU (red) and DAPI (blue). Quantification of % BrdU labeled cells are shown on the right panel. $BrdU^+$-cells are normalized to the total DAPI-stained nucleus in the field. (F-G) Relative fold change of mRNA (F) and % BrdU labeled nuclei (G) of NRV cFbs transfected with control or Cilp1 siRNA. Longer BrdU labeling time (50 min) were used in (G). (H) % BrdU-labeled cells in adult cFbs treated with vehicle or recombinant CILP1 protein. (I) Relative mRNA of adult cFbs transfected with control or Cilp1 siRNA. Error bars are SEM. (A, E, F-I) * $p< 0.05$ by student t test. D, Mann-Whitney test. ns: not significant.

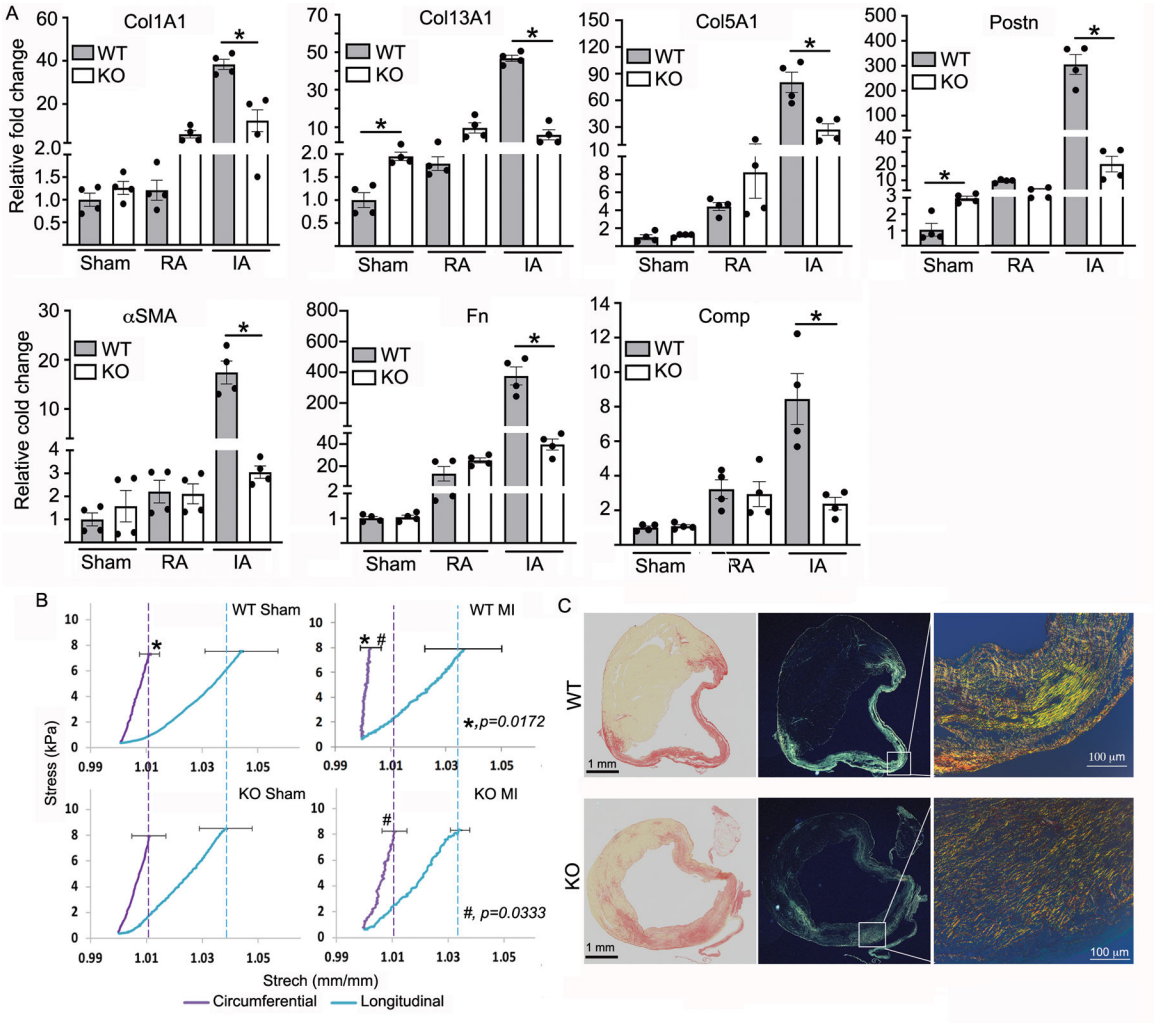

Figure 7. Cilp1 regulates collagen remodeling.

(A) Relative fold change of collagen genes and fibrosis-related genes in sham and post-MI day 7 WT and *Cilp1* KO hearts. (B) Biaxial mechanical testing of sham and post-MI day 7 WT and *Cilp1* KO hearts (n=4–6). (C) Representative PSR staining (left panel) and birefringent image (middle and right panels) of WT and *Cilp1* KO heart at post-MI day 7. ∗; # $p<0.05$ by student t test.

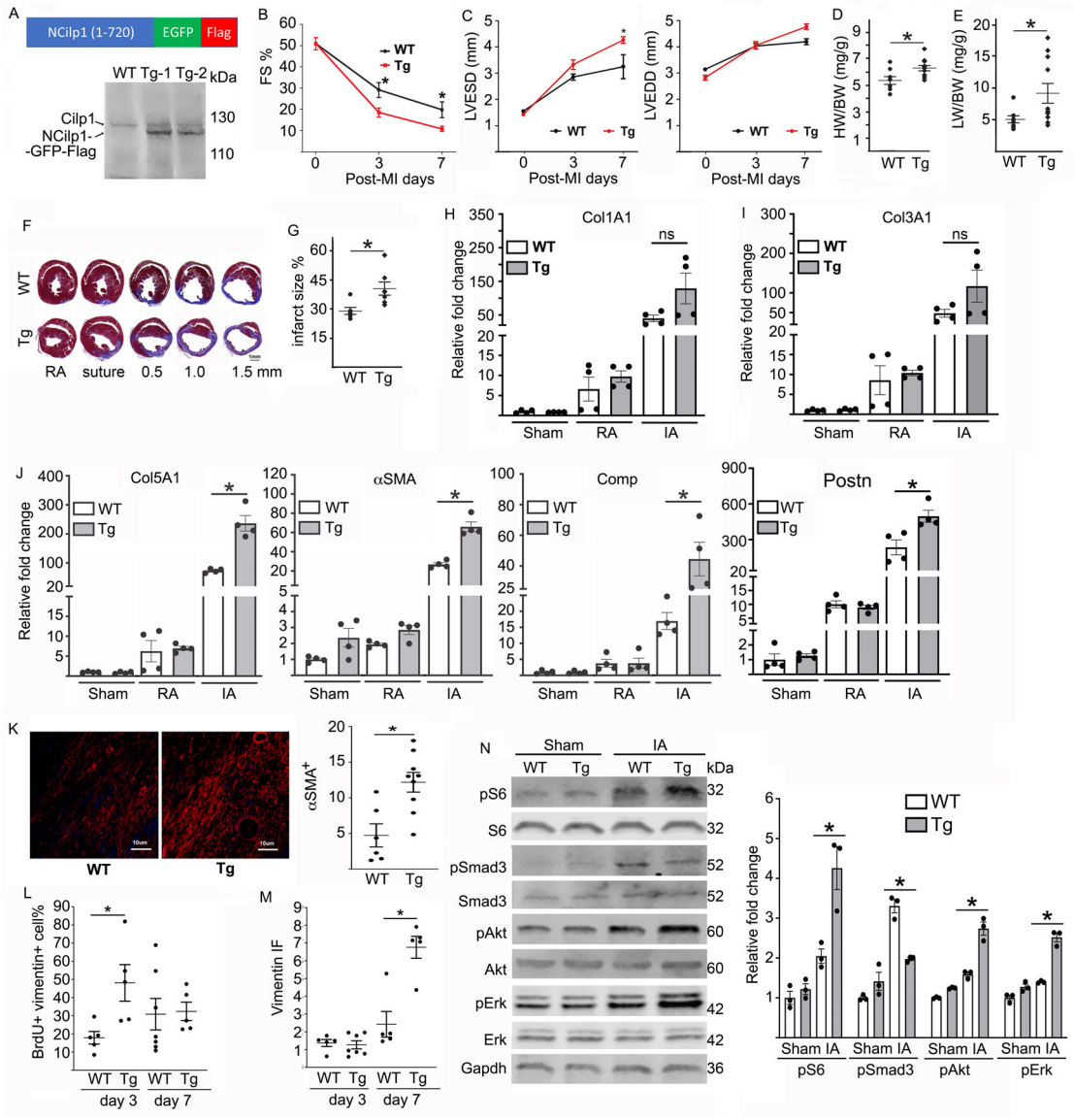

Figure 8. Overexpression of Cilp1 in myofibroblasts exacerbates post-MI cardiac remodeling and myofibroblast proliferation.

(A) Schematic of NCilp1 transgene (upper panel) and western blot of endogenous Cilp1 and NCilp1-GFP in infarcted WT and Tg hearts. (B-C) fractional shortening (FS %) (B), LVESD and LVEDD (C) of post-MI WT and Tg mouse hearts. (D-E) HW/BW and LW/BW of infarcted WT and Tg hearts at post-MI day 7. (F) Representative Trichrome-stained histological section of infarcted WT and Tg hearts at post-MI day 7. (G) Quantification of infarct size from heart sections in (F). (H-J) Relative mRNA from IA and RA of WT and Tg hearts at post-MI day 7. (K) Representative aSMA-stained immunofluorescence micrograph of WT and Tg hearts at post-MI day 7 in the IA. Immunofluorescence were quantified and normalized to the IA (right panel). WT and Tg mice were pulse-labeled with BrdU (ip, 60 mg/kg) for 4 hrs at post-MI day 3 and 7. Heart sections were co-stained with antibodies against BrdU and vimentin. % BrdU labeled vimentin^{+} cells (L) and vimentin immunofluorescence normalized to the IA (M) were quantified. Error bars are SEM, *, $p <$

0.05. (K) Representative western blot of indicated proteins from sham and IA of WT and Tg hearts at post-MI day 3. Quantifications of the band intensity from the western blot were shown on the right. n=3. Error bars are SEM. (B-D, G, J-L, N) * $p<0.05$ by student t test. (H, I, M) * $p<0.05$ by Mann-Whitney test. ns: not significant.